

INSAR PHASE PROFILES AT BUILDING LOCATIONS

A. Thiele^{a,*}, E. Cadario^a, K. Schulz^a, U. Thoennessen^a, U. Soergel^b

^a FGAN-FOM, Research Institute for Optronics and Pattern Recognition, Gutleuthausstrasse 1,
D-76275 Ettlingen, Germany - (thiele, cadario, schulz, thoennessen)@fom.fgan.de

^b Institute of Photogrammetry and GeoInformation, Leibniz Universität Hannover, Nienburger Strasse 1,
D-30167 Hannover, Germany - soergel@ipi.uni-hannover.de

Commission VI, WG III/4

KEY WORDS: Interferometry, SAR, Building Recognition

ABSTRACT:

The improved ground resolution of state-of-the-art synthetic aperture radar (SAR) sensors suggests utilizing SAR data for the analysis of urban areas. Building recognition however suffers from the consequences of the inherent side-looking viewing geometry of SAR, particularly occlusion and layover hinder the analysis. Usually extracted layover regions are not considered further in the recognition workflow. However, since layover regions contain information mixture of the building and its surrounding area, it is worthwhile to make efforts to understand such signal in order to tell different contributions of building façade and roof apart from those of other objects aiming at improvement of recognition.

Considering InSAR data conspicuous phase distributions at building locations are observable. The concerned area begins always at the building parts facing the sensor, in extreme cases even the entire data of the building area is inferred by layover. The characteristics of the phase profile in range direction depend on sensor and illumination properties as well as on geometric attributes of buildings. The processed interferometric phase information of a single range cell may result from superposition of several signal contributions of backscatters with same range distance to the sensor.

In this paper, a model is presented to calculate the expected interferometric phase values based on a given surface profile. The process takes into account that a mixture of several contributions defines the interferometric phase of a single range cell. Based on this model, simulations shall be included in an iterative analysis-by-synthesis approach for building recognition from multi-aspect InSAR data. The focus of the proposed model is to understand the impact of the building's geometry on the phase profiles, material properties are not considered in the present state. The assessment process of the simulated phase profiles is performed by comparison with real InSAR data, based on phase values of single range lines.

1. INTRODUCTION

The recognition of buildings from SAR data is often driven by analysis of magnitude images focussing on effects caused by the inherent oblique scene illumination, such as layover, radar shadow and multipath signal propagation (Simonetto et al., 2005), (Thiele et al., 2007). If InSAR data are provided, they are basically used for orthorectification and height estimation of the building hypotheses (Bolter, 2001), (Gamba et al., 2003). Due to the signal mixture in layover areas, at first glance the related InSAR elevation data often seem to exhibit arbitrary height values between ground and rooftop levels. Because of this fact, layover areas are often excluded from further recognition steps. In former research work conspicuous InSAR phase profiles at building locations were observable, which permitted the question of including this data in the process of building recognition and reconstruction. A prerequisite for exploiting layover signal is an understanding how different scattering objects contribute to the given InSAR data, which can be achieved for example based on simulation.

The analysis of InSAR phases in (Burkhart et al., 1996) was motivated by the task of building and tree extraction. The focus was on removal of noise and artefacts from the InSAR data. The appearance of the layover area in InSAR phase data at buildings was referred as "front porch". (Bickel et al., 1997) as well investigated mapping of building structures into InSAR

heights and coherence data, and presented ideas to identify and avoid the layover problem. A study of the joint statistic of SAR images concentrating on layover areas was published in (Wilkinson, 1998).

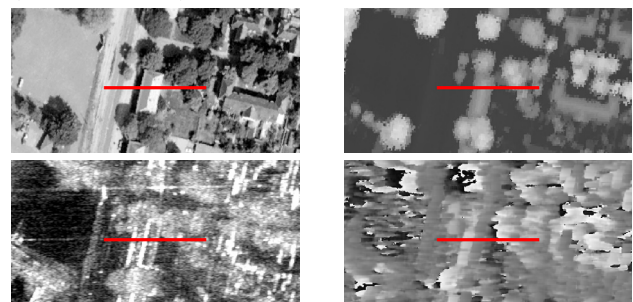


Figure 1. Appearance of gable-roofed building in orthophoto (u.l.), LIDAR DSM (u.r.), SAR magnitude image (l.l.), and InSAR phase image (l.r.); Red line marks range profile

In (Petit et al., 2000) an interferogram simulator was presented to reproduce and study coherence losses for steep gradient relief. The studies of (Cellier et al., 2006) are focused on segmentation of the borderline of the layover area as seen from the sensor, in order to determine the building's height. An interferometric mixture model using two contributors was developed and used to improve the estimation of the frontage height of an industrial building.

* Corresponding author. This is useful to know for communication with the appropriate person in cases with more than one author.

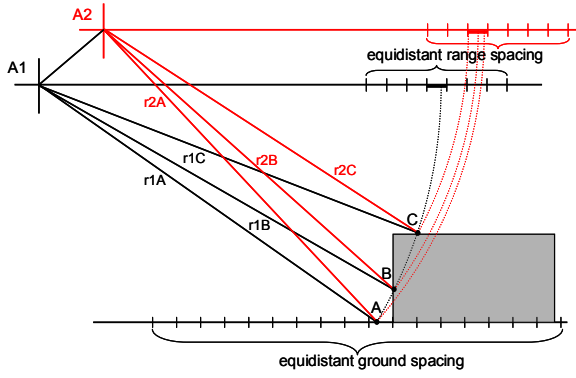


Figure 2. Contribution distribution of InSAR measurements at building location

An analysis of the full layover area is necessary to clarify whether the InSAR phase profiles in range direction include useful information for the reconstruction of buildings. In Figure 1 an image example is given. The red line marks a profile, which is analyzed in the following.

The first step of studying the potential of phase profiles for recognition is simulation of interferometric phases, which takes all contributors into account. In this paper an appropriate phase mixture model is proposed. Results for different building types are presented and compared with real InSAR data. The analysis is mainly focused on the layover area.

2. PHASE PROFILE MODELLING

2.1 Definition and Implementation of Phase Mixture Model

For across-track SAR Interferometry two SAR images are required, which were taken separated by a baseline perpendicular to sensor tracks. After SAR processing the incoming signals gathered by antennas A1 and A2 are mapped into the related range/azimuth resolution cells (pixel) S_1 respectively S_2 of the complex SAR images. The signal phasor represented by a certain resolution cell is modelled to be the result of coherent superposition of contributions of every individual scattering object inside the related 3d volume. Equation 1 describes this superposition for a constellation depicted in Figure 2.

$$\begin{aligned} S_1 &= a_1 \cdot e^{j\varphi_1} \\ &= a_{1A} \cdot e^{j\varphi_{r1A}} + a_{1B} \cdot e^{j\varphi_{r1B}} + a_{1C} \cdot e^{j\varphi_{r1C}} \\ S_2 &= a_{2A} \cdot e^{j\varphi_{r2A}} + a_{2B} \cdot e^{j\varphi_{r2B}} + a_{2C} \cdot e^{j\varphi_{r2C}} \end{aligned} \quad (1)$$

where: a_{1n}, a_{2n} = magnitude of contributor n
 $\varphi_{r1n}, \varphi_{r2n}$ = phase of contributor n

In a simplified manner SAR can be described as distance measurement in horizontal cylinder coordinates with high resolution in radial (range) and azimuth coordinates, but poor resolution in off-nadir angle (elevation) direction. The latter is the reason for the layover phenomenon.

An example for a building is given in Figure 2. The point A (ground level), point B (building wall) and point C (building roof) have the same distance ($r_{1A} = r_{1B} = r_{1C}$) to antenna A1. But, related to antenna A2 the range distances differ ($r_{2A} \neq r_{2B} \neq r_{2C}$): point C is closest to the sensor, followed by point B and point A.

Since the layover effect is modelled to be independent from azimuth, but off-nadir angle θ rises over swath with increasing range, the simulation is carried out along range profiles.

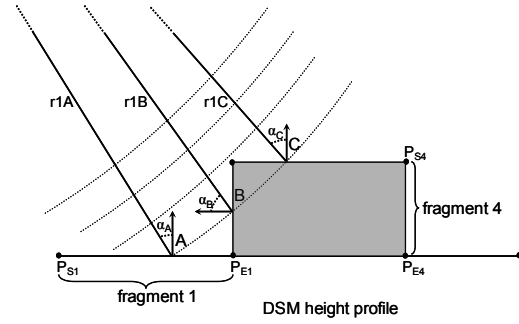


Figure 3. DSM profile of a flat-roofed building based on fragments; local incidence angle of radar signal

From the phase difference of the two complex images the InSAR phase data is calculated. In the simulation different signal contributions at elevation discontinuities especially related to building locations are considered:

$$\begin{aligned} S &= S_1 \cdot S_2^* = a_1 e^{j\varphi_1} \cdot a_2 e^{-j\varphi_2} = a_1 a_2 \cdot e^{j(\varphi_1 - \varphi_2)} \\ &= (a_{1A} \cdot e^{j\varphi_{r1A}} + a_{1B} \cdot e^{j\varphi_{r1B}} + a_{1C} \cdot e^{j\varphi_{r1C}}) \cdot \\ &\quad (a_{2A} \cdot e^{-j\varphi_{r2A}} + a_{2B} \cdot e^{-j\varphi_{r2B}} + a_{2C} \cdot e^{-j\varphi_{r2C}}) \end{aligned} \quad (2)$$

The process of the phase profile modelling starts with the definition of the sensor parameters, e.g. wavelength, sensor altitude, antenna configuration, slant range resolution. From a given ground truth DSM range profiles are derived, in which linear patches are segmented (synthetic DSM). An example for a flat-roofed building is depicted in Figure 3. In the next step the synthetic DSM is split into DSM fragments in ground range of approximate constant gradient, with $P_S (x_S, y_S, z_S)$ as start point and $P_E (x_E, y_E, z_E)$ as end point. For each of these ground fragments the corresponding range cells are determined and the following quantities per range cell are calculated: local incidence angle α_i between radar signal path and normal vector n_i (equation 3), range distance difference Δr_i and phase difference $\Delta \varphi_i$ (equations 4).

$$\cos \alpha_i = \frac{(A_1 - P_i) \cdot n_i}{|(A_1 - P_i)| \cdot |n_i|} \quad (3)$$

$$\begin{aligned} \Delta r_i &= |A_1 - P_i| - |A_2 - P_i| \\ \Delta \varphi_i &= -2\pi \cdot \frac{\Delta r_i}{\lambda} \end{aligned} \quad (4)$$

where: P_i = point coordinate vector
 A_1, A_2 = antenna vector
 λ = wave length

The simulation is carried out in the range grid of the final interferogram. In this manner no co-registration of the two SAR images is required. The simulated interferometric phases are calculated by summing up all contributions of one range cell. Equation 5 describes the interferogram calculation for m backscatter contributors with the assumption of equal magnitude a:

$$S = m \cdot a \cdot \sum_m a \cdot e^{j\Delta \varphi_m} \quad (5)$$

Considering additionally the local incidence angle α_i leads to equation 6 for the interferogram calculation.

$$S_{\alpha} = \sum_m \cos \alpha_m \cdot a \cdot \sum_m \cos \alpha_m \cdot a \cdot e^{j\Delta\varphi_m} \quad (6)$$

The process of phase profile modelling includes detection of shadow areas and flat earth correction. The shadow areas are modelled with a reflectivity of zero without implementing a noise contribution.

2.2 Examples of Simulated Phase Profiles

The influence of viewing geometry parameters is discussed for two simple building models: flat-roofed and gable-roofed. The first row in Figure 4 shows synthetic DSM profiles of a flat- (left) and a gable-roofed (right) building. The number of different contributors for a single range cell is given in the second row of Figure 4. The simulated phase profiles considering local incidence angle of radar signal are shown in the third row. In the fourth row additionally the component of flat earth correction is also considered at locations without backscatter contributors like shadow regions. In real InSAR data these regions are characterized by a random phase distribution, which is e.g. accounted in the model of (Wilkinson, 1998).

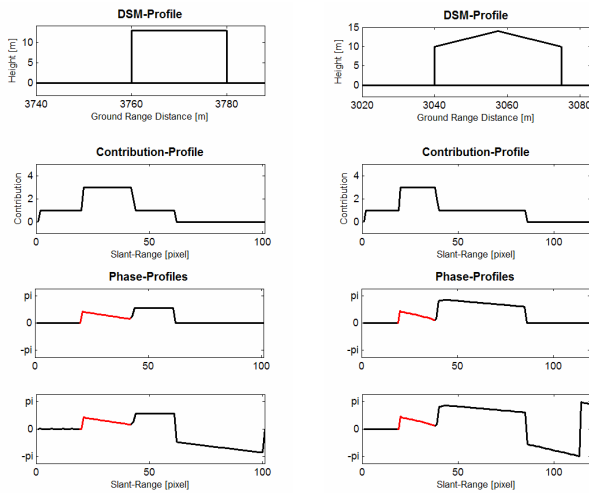


Figure 4. Simulation of phase profiles at flat- and gable-roofed buildings; Layover area marked red

The impact of the local incidence angle α of the radar signal is essential for the mapping of certain buildings. To emphasize this in Figure 5 simulated phase profiles of a gable-roofed building are given assuming off-nadir angle θ of 35° (left) respectively 50° (right). The profiles display the highest differences in front of the building at the layover area. The steepest off-nadir angle (35°) shows the highest difference (equation 3, 6).

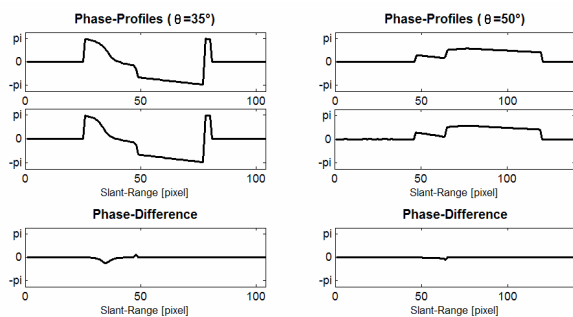


Figure 5. Simulation neglecting (top) and considering (middle) local incidence angle α , bottom: difference middle-top

Beside the local incidence angle of the radar signal other quantities affect the appearance of the InSAR phase profiles. That includes sensor parameters (e.g. range resolution and antenna configuration), illumination parameters (e.g. range distance and off-nadir angle), and building model parameters (e.g. height, width and roof type). The here presented studies are focused on the impact of illumination and building model parameters. In Figure 6 simulated phase profiles are shown for a flat-roofed building (10 m height and 40 m width) as a function of the off-nadir angle in the range from 20° up to 50° . The distribution of the phase information of the layover area as well as the roof part includes salient phase jumps to values lower zero. That is caused by the ambiguity height Δh_i defined by:

$$\Delta h_i = \lambda \frac{r_i \cdot \sin \theta_i}{B_{\perp}} \quad (7)$$

where: B_{\perp} = perpendicular component of the baseline
 r_i = range distance to position i
 θ_i = off-nadir angle on position i

For the simulated configuration the ambiguity height is given from 8 m (20°) up to 24 m (50°). Accordingly, with a scaling from $-\pi$ up to π and terrain definition at scale point zero, only the half of the elevation interval can be used for a positive display of building phases. Furthermore, the maximum phase value in the layover area is approximately building phase.

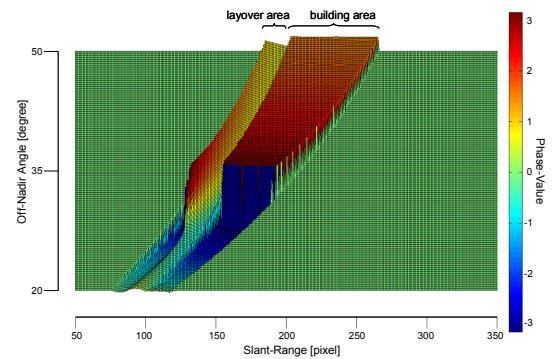


Figure 6. Changes in simulated phase profile for flat-roofed building by varying off-nadir angle

Analogue studies have been undertaken for a gable-roofed building (8 m eaves height, 12 m ridge height, 50 m width leading to 10 degree roof pitch). In addition building size respectively roof pitch are varied. The phase schemas are given in Figure 7. The influence of varying the off-nadir angle from 20° up to 50° is shown in Figure 7a. As mentioned before, a steeper off-nadir angle leads to a smaller 2π unambiguous elevation interval (equation 7), which results in phase profile values lower zero.

The variation of the building size from 10 m up to 70 m yields to a change of the roof pitch from 40° down to 7° , the simulated profiles are depicted in Figure 7b. The first profile (at 10 m) reveals no exclusive phase signature of the roof at all, the entire roof signal is compound with other contributions in the layover area. With growing building width exclusive phase signature of the roof is observable, but after a certain building size the above mentioned phase wrapping takes effect. For small buildings this behaviour is not observed, because of the layover phenomenon. In comparison with Figure 7a is the 2π unambiguous elevation interval for Figure 7b constant.

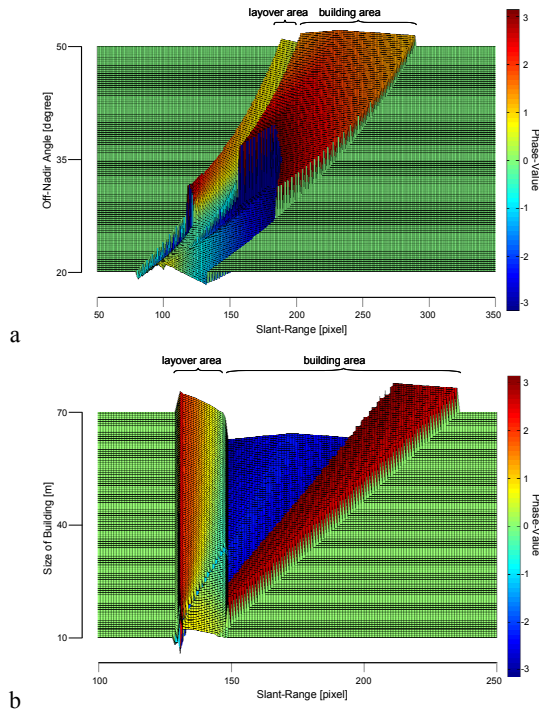


Figure 7. Changes in simulated phase profile for gable-roofed buildings by varying off-nadir angle (a) and building size (b)

This observation is confirmed by comparison with real InSAR data; especially in large urban areas with similar building inventory illuminated under different off-nadir angles.

Even if the building's height is smaller than the unambiguous elevation interval, this effect may occur due to suboptimal choice of the elevation interval borders in the InSAR processing. In such cases a phase shifting procedure is beneficial. This step contains phase shifting upwards by 2π for all phase values significantly below a threshold.

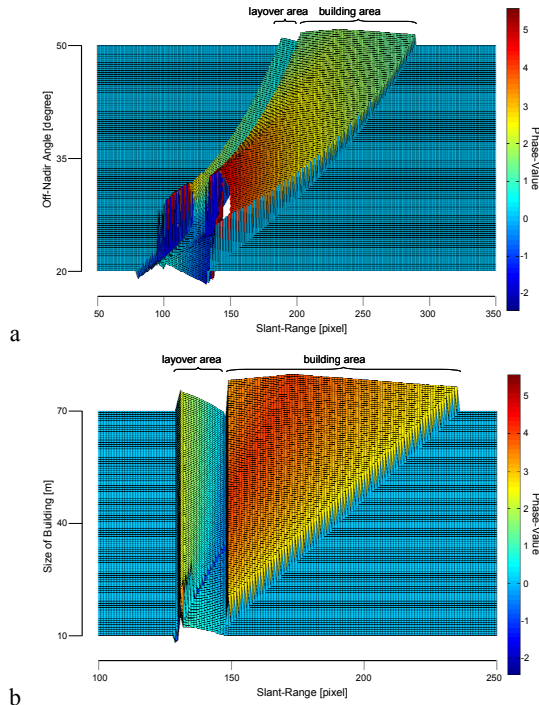


Figure 8. Changes in simulated phase profile for gable-roofed building by varying off-nadir angle (a) and building size (b) after phase shifting operation

The new results, including such a phase shifting, for both parameter variations (off-nadir angle respectively building size) are given in Figure 8. The described phase shifting is obviously helpful for the example of building size variation (Figure 8b). However, considering Figure 8a this procedure is less helpful, because the 2π unambiguous elevation interval connected to steep off-nadir angles is too small for an unambiguous visualisation of the phase values.

3. PHASE PROFILES IN REAL INSAR DATA

3.1 Calculation of Interferogram

The calculation of the interferometric phase values based on the SLC data of both antennas is done in slant range geometry. Due to the baseline established by the geometric separation of the antennas, the two SAR images have different range/azimuth coordinate grids. Therefore, co-registration is required. Since InSAR relies on the phase difference of the two given complex SAR images, sub-pixel accuracy is a prerequisite.

The subsequent interferogram generation includes multi-look filtering, followed by flat earth correction and phase centring. By phase centring a phase distribution with zero mean is achieved in the manner of the model results to make the comparison of both phase profiles possible. For some cases subsequent phase shifting is useful to reduce phase ambiguities at building locations.

3.2 Examples of Real Phase Profiles

The investigated SLC InSAR data set was produced by Intermap Technologies (Schwaebisch et al., 1999), and have a spatial resolution of about 38 cm in range and 16 cm in azimuth direction. The two X-Band sensors operated with effective baseline $B \approx 2.4$ m. The 2π unambiguous elevation span is about 16 m in close range and 20 m in far range. The mapped area is characterized by a mixture of residential and industrial building structures.

A small subset of this InSAR data set as well as the corresponding ground truth data (orthophoto, LIDAR DSM) are shown in Figure 9. The red line in the images signalizes the range profile chosen for the subsequently tests.

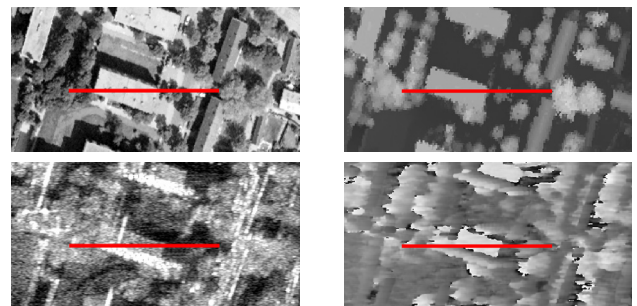


Figure 9. Appearance of flat-roofed building in orthophoto (u.l.), LIDAR DSM (u.r.), SAR magnitude image (l.l.), and measured InSAR phase image (l.r.); Red line marks range profile

For the investigation of typical measured phase profiles the influence of the multi-look window size was studied. The effects of window size $[1 \times 1]$ (single look), $[3 \times 3]$, $[5 \times 5]$ and $[9 \times 9]$ are illustrated for the chosen range profile in Figure 10 (the first image on top shows the corresponding LIDAR DSM profile).

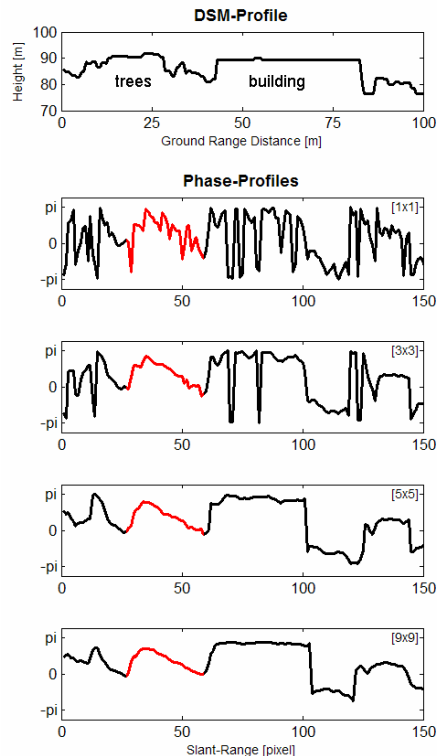


Figure 10. LIDAR DSM profile and corresponding measured InSAR phase profiles based on different multi-look parameters; Layover areas are marked red

Obviously, smoothing of the phase values to some extent is advisable, which can be confirmed with respect to the building recognition task from real InSAR data. For the following comparison between simulated and measured phase profiles the [9x9] interferogram was chosen.

In Figure 11 the measured InSAR phase profiles of a flat-roofed (left) and a gable-roofed (right) building are shown. The layover area (marked red) shows the previously discussed “front-porch” shape (Burkhart, 1996), because in this area the different heights of the contributors for the same range cell are mixed. After the initial maximum height value arising from dominate signal of the roof corner structure, usually a declining trend is observed towards the corner reflector spanned by the wall and the ground in front at the end of the layover region, which in theory should coincide with terrain level, but in reality sometimes larger elevation values are observed.

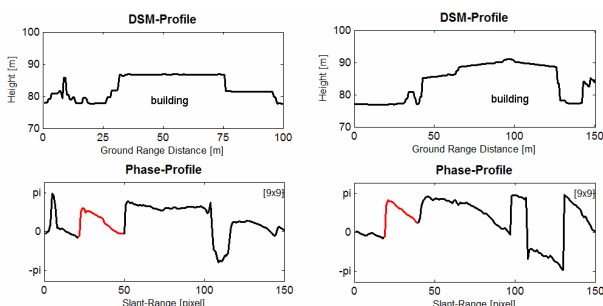


Figure 11. LIDAR DSM profiles and corresponding measured InSAR phase profiles; Layover area marked red

The typical distribution of InSAR profiles is not restricted to the investigated data set or sensor set-up. Similar phase contributions at building locations especially in the layover

areas are observable also for other SAR sensors, baseline configurations and range resolutions.

4. COMPARISON OF PHASE PROFILES

The assessment of the simulated phase and the real InSAR interferograms is based on comparison of phase profiles in range direction. Therefore, a suitable LIDAR DSM profile of the scenery was selected and generalized (synthetic DSM) for the modelling process preserving geometrical dimensions and other key features (e.g. roof type of building). The modelled physical parameters (e.g. wavelength, length of baseline and sensor altitude) are extracted from log files of the investigated InSAR data set.

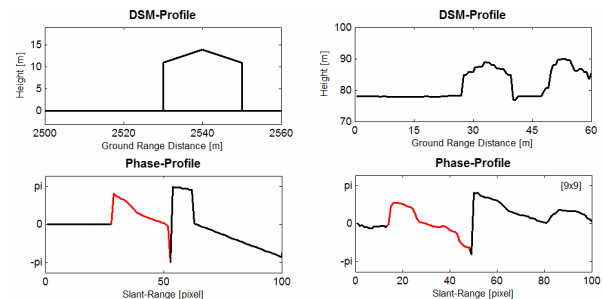


Figure 12. Synthetic DSM profile and simulated phase profile (left column); LIDAR DSM profile and measured InSAR phase profile (right column); Layover area marked red

The first comparison in Figure 12 shows the simple gable-roofed building also visualized in Figure 1. The simulation yields sharper edges and crisper contours. This is due to the generalisation effect of the model and the neglect of material properties.

The sensor-close part of the phase profiles match better then on the rear part. This difference is caused by phase noise from occlusion and interference from adjacent trees. The phase peaks below zero of both phase profiles could be compensated by the step of phase shifting. Focused on the layover area similarities are observable especially at the highest and lowest point of the area. The comparison of phase information in the shadow area is not reasonable, because the simulated phase profile only shows the flat earth component without apparent layover of the trees as observable in the measured phase profile.

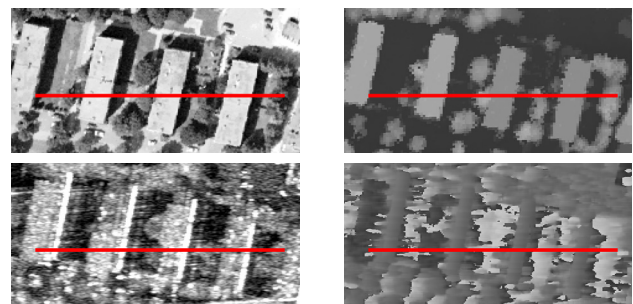


Figure 13. Appearance of flat-roofed building row in orthophoto (u.l.), LIDAR DSM (u.r.), SAR magnitude image (l.l.), and InSAR phase image (l.r.); Red line marks range profile

A more complex scenery is illustrated in Figure 13. The red line marks the location of the following investigated slant range profiles. The related synthetic and ground truth elevation data as well as simulated and measured phase profiles are depicted in Figure 14. The scene consists of a group of flat-roofed buildings of different height. Direct comparison of the phase

profiles is complicated by the interference between the neighbouring buildings and trees in-between. Furthermore, the interpretation is hampered by the 2π steps in the measured phase profile.

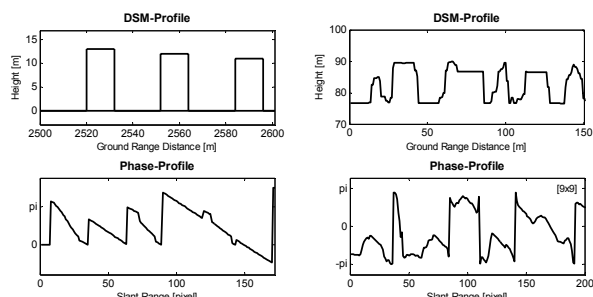


Figure 14. Synthetic DSM profile and simulated phase profile (left column); LIDAR DSM profile and measured InSAR phase profile (right column)

A similar configuration of gable-roofed buildings is given in Figure 15. The group of five buildings is characterised by four buildings of same and one of opposite orientation. In the generalised synthetic DSM, this building is replaced as a flat-roofed building (Figure 16).

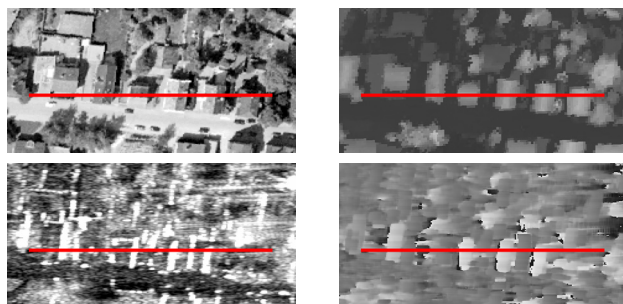


Figure 15. Appearance of gable-roofed building row in orthophoto (u.l.), LIDAR DSM (u.r.), SAR magnitude image (l.l.), and InSAR phase image (l.r.); Red line marks range profile

The simulated phase profiles in this case match even better the measured phase profile compared to the flat-roofed building row (Figure 14). The main reason is probably the absence of tall trees. Similarities are observable at significant points of the layover areas as well as in the phase distribution in the layover areas.

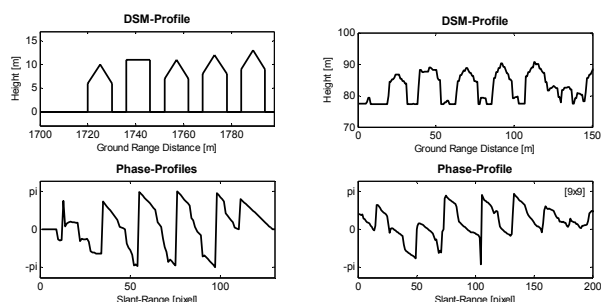


Figure 16. Synthetic DSM profile and simulated phase profile (left column); LIDAR DSM profile and measured InSAR phase profile (right column)

The sets of simulated and measured phase profiles reveal, how complex the analysis of the layover area is, especially if mutual interference caused by trees and closed neighbouring buildings have to be taken into account.

5. CONCLUSION

In this paper a model was proposed to simulate the interferometric phase values, based on a given surface profile. The simulation approach is tailored to the needs of an iterative analysis-by-synthesis approach for building recognition. The process takes into account that several scattering processes can contribute to the interferometric phase of a single range cell. Material properties are not considered, because such data is usually not available for the building recognition task. The influence of a number of different parameters was discussed. The model was verified by comparison with real InSAR data. The analysis focussed on the phase distributions in the layover area at building locations. The high correlation between simulated and real InSAR phase profiles fosters further investigations how such simulations can be best exploited in a frame work for building recognition and reconstruction. Furthermore an automatic phase unwrapping at building locations for disadvantageous 2π unambiguous elevation intervals is a crucial step and will be investigated in future work to improve the building reconstruction frame work.

6. REFERENCES

- Bickel, D.L., Hensley W.H., Yocky, D.A. 1997. The Effect of Scattering from Buildings on Interferometric SAR Measurements. In: *Proceedings of IGARSS*, Vol. 4, 3-8 August, Singapore, pp. 1545-1547.
- Bolter, R. 2001. Buildings from SAR: Detection and Reconstruction of Buildings from Multiple View High Resolution Interferometric SAR Data. Ph.D. dissertation, University Graz.
- Burkhart, G.R., Bergen, Z., Carande, R. 1996. Elevation Correction and Building Extraction from Interferometric SAR Imagery. In: *Proceedings of IGARSS*, Vol. 1, 27-31 May, Lincoln, Nebraska, USA, pp. 659-661.
- Cellier, F., Oriot, H., Nicolas, J.-M. 2006. Study of altimetric mixtures in layover areas on high-resolution InSAR images. In: *Proceedings of EUSAR*, Dresden, Germany, CD ROM.
- Gamba, P., Dell'Acqua, F., Houshmand, B. 2003. Comparison and fusion of LIDAR and InSAR digital elevation models over urban areas. In: *International Journal Remote Sensing*, Vol. 24, No. 22, 20 November, pp. 4289-4300.
- Petit, D., Adragna, F. 2000. A new interferogram simulator: 2SIR. Study of coherence losses for tortured reliefs. In: *Proceedings of SAR Workshop: CEOS - Working Group on Calibration and Validation*, ESA-SP Vol. 450, 26-29 October 1999, Toulouse, France, p.591.
- Schwaebisch, M., Moreira, J. 1999. The high resolution airborne interferometric SAR AeS-1. In: *Proceedings of the Fourth International Air-borne Remote Sensing Conference and Exhibition*, Ottawa, Canada, pp. 540-547.
- Thiele, A., Cadario, E., Schulz, K., Thoennessen, U., Soergel, U. 2007. Building Recognition from Multi-Aspect High Resolution InSAR Data in Urban Area. In: *IEEE Transactions on Geoscience and Remote Sensing, EUSAR Special Issue 2006*, in press.
- Wilkinson, A. J. 1998. Synthetic Aperture Radar Interferometry: A Model for the Joint Statistics in Layover Areas. In: *Proceedings of COMSIG*, 7-8 September, Rondebosch, South Africa, pp. 333-338.